

Coupled Joint PDF and Spray Flamelet Modeling for Methanol and Ethanol/Air Spray Combustion

Hai-Wen Ge¹, Eva Gutheil^{2*}

¹Engine Research Center, University of Wisconsin-Madison,
1500 Engineering Drive, Madison, WI 53706, USA.

²Interdisziplinäres Zentrum für Wissenschaftliches Rechnen, Universität Heidelberg,
Im Neuenheimer Feld 368, 69120 Heidelberg, Germany.

Abstract

A joint mixture fraction - enthalpy probability density function (PDF) is proposed for the simulation of turbulent spray flames. The Interaction-by-Exchange-with-the-Mean (IEM) model for gas-phase flows is extended to describe the molecular mixing in both non-reactive and reactive spray flows. Standard spray and turbulence models are used to describe the remaining gas flow characteristics and the liquid phase. The spray flamelet model is implemented to treat the detailed chemical reactions. Results for methanol/air and ethanol/air spray flames are compared with both experiment and previous RANS computations.

Introduction

Liquid fuels are used in practical combustion systems such as internal combustion engines, gas turbines, liquid-fueled rockets, and they significantly contribute to our energy supply. The combustion efficiency, combustion stability, and pollutant formation of these systems strongly depend on the character of the turbulent spray, and an improved understanding of turbulent spray combustion systems is required.

The PDF (probability density function) method is a powerful tool to investigate turbulent non-reactive and reactive flows. It treats the chemical reaction source term without any assumptions on turbulent fluctuations [1-4]. Therefore, the PDF method is very attractive for turbulent combustion modeling. They are a very active and fruitful research area [5]. PDF methods were introduced into the field of multiphase flows in the beginning of the 1990's. They were used to describe the dispersed phase [6], gas phase [7-12], or all liquid-phase and gas-phase random variables [13-16]. For the reactive cases, only Taut et al. [11] used detailed chemistry. Others [7,10,12] employed one-step global reaction mechanism.

In the authors' previous work, a single scalar PDF [18] and a joint velocity-scalar PDF [19] were proposed for the simulation of turbulent non-reactive spray flows. The latter PDF aims to improve the velocity prediction of the spray flow.

The present work concerns a joint enthalpy-mixture fraction PDF is developed to simulate the turbulent spray flames. Chemical reactions are implemented through use of the spray flamelet model [17] for turbulent combustion, where spray flamelet libraries for methanol/air and ethanol/air combustion are implemented.

The numerical results are compared with both experimental data and former Reynolds-averaged

Navier-Stokes (RANS) simulations and with experimental results.

Mathematical Model

We define an one-point one-time Eulerian, mass-weighted joint probability density function (PDF), $\tilde{f}(\Phi; \vec{x}, t)$, for the gas phase of turbulent spray flows:

$$\tilde{f}(\Phi; \vec{x}, t) = \rho(\Phi) \langle \delta(\Phi - \Psi) \rangle / \langle \rho \rangle \quad (1)$$

where Φ and Ψ are the vector of characteristic variables in sample space and state space, respectively; ρ is the gas density. The transport equation of the PDF is written as:

$$\frac{\partial \langle \rho \rangle \tilde{f}}{\partial t} + V_i \frac{\partial \langle \rho \rangle \tilde{f}}{\partial x_i} = - \langle \rho \rangle \frac{\partial}{\partial \Psi_i} \left(\left\langle \frac{d\Phi_i}{dt} \middle| \Psi \right\rangle \tilde{f} \right) \quad (2)$$

where V_i is the gas velocity in the sample space. In the present work, a joint enthalpy - mixture fraction PDF, $\Phi = (H, \xi_C)^T$, is proposed for reactive spray flows.

The corresponding transport equation is:

$$\begin{aligned} \frac{\partial \langle \rho \rangle \tilde{f}}{\partial t} + V_i \frac{\partial \langle \rho \rangle \tilde{f}}{\partial x_i} + \frac{\partial \langle S_{i,1} \rangle \tilde{f}}{\partial \xi_C} + \frac{\partial \langle S_{i,h} \rangle \tilde{f}}{\partial \eta} = \\ - \frac{\partial}{\partial \xi_C} \left[\left\langle \frac{\partial}{\partial x_j} \left(\Gamma_M \frac{\partial \xi_C}{\partial x_j} \right) \middle| \xi_C, \eta \right\rangle \tilde{f} \right] - \frac{\partial}{\partial \eta} \left[\left\langle \frac{\partial}{\partial x_j} \left(\Gamma_h \frac{\partial h}{\partial x_j} \right) \middle| \xi_C, \eta \right\rangle \tilde{f} \right] \end{aligned} \quad (3)$$

where V_i is the gas velocity in the sample space; $S_{i,1}$ and $S_{i,h}$ are the source terms due to spray evaporation;

Γ_M and Γ_h are the mass and energy exchange coefficients, respectively. The terms on the left hand side appear in closed form, including the terms of time derivative, convection, and spray sources for the total mass, $\langle S_{i,1} \rangle$, and for enthalpy, $\langle S_{i,h} \rangle$. The terms on the right hand side represent the molecular diffusion flux of mixture fraction and enthalpy in sample space, which depend on the multi-point information; they need

* Corresponding author: gutheil@iwr.uni-heidelberg.de
Associated Web site: <http://www.iwr.uni-heidelberg.de/groups/mfc/>
Proceedings of the 21th ILASS - Europe Meeting 2007

to be modeled. In the present work, the interaction-by-exchange-with-the-mean (IEM) model [18] is used which is extended to account for interaction of the gas with the spray. The evolution equation of mixture fraction and enthalpy is written as:

$$\frac{d\tilde{\xi}_c^*(t)}{dt} = -\frac{1}{2} \frac{\tilde{\varepsilon}}{\tilde{k}} C_\phi \left[\tilde{\xi}_c^*(t) - \tilde{\xi}_c \right] + \frac{\langle S_{l,1} \rangle}{\langle \rho \rangle} \quad (4)$$

$$\frac{dh^*(t)}{dt} = -\frac{1}{2} \frac{\tilde{\varepsilon}}{\tilde{k}} C_\phi \left[h^*(t) - \bar{h} \right] + \frac{\langle S_{l,h} \rangle}{\langle \rho \rangle} \quad (5)$$

The last terms in Eqs. (4) and (5) account for the interaction with the spray.

The present joint enthalpy – mixture fraction PDF transport equation is solved using a Monte-Carlo/Lagrangian particle method. Mean variables appearing in the PDF transport equation are supplied by the RANS method and the spray computation. Physical models include extended $k-\varepsilon$ model for turbulent spray flows, Abramzon-Sirignano model, stochastic separated flow (SSF) model, and infinite-conductivity model for droplets. The RANS method, spray models, and corresponding numerical method are described in detail in [20]. With the Monte-Carlo/Lagrangian particle method, the gas flow is discretized into a large number of gas particles. Each gas particle has the properties of (m^*, \bar{x}^*, Φ^*) , which are the mass, position, and considered quantities (mixture fraction and enthalpy), respectively. The evolution of the Lagrangian particles is tracked. Numerical issues of the Monte-Carlo method are detailed in [18].

Detailed chemical reaction mechanisms are implemented through a spray flamelet model [17]. In the present work, it consists of 23 species and 168 elementary reactions for methanol/air combustion, and 38 species and 337 elementary reactions for the ethanol/air system. The laminar spray flamelet library has been pre-calculated for counterflow spray flames [21,22]. Each flamelet is characterized by the mixture fraction and its dissipation rate as well as initial droplet size, initial droplet velocity, and equivalence ratio. Dirac-Delta functions are assumed for the initial droplet size, initial droplet velocity, and equivalence ratio. The instantaneous dissipation rate of a gas particle is sampled from a logarithmic-normal distribution. Then the compositions of this gas particle are determined by linear interpolation of the data stored in the spray flamelet library. Furthermore, the temperature of this gas particle is computed from its enthalpy and its composition. Thus, the gas particles contain information of mass, mixture fraction, enthalpy, composition, and temperature. The mean variables are evaluated as the mass-averaged value of the gas particles' property.

Results and Discussion

A joint enthalpy and mixture fraction PDF model is used to simulate both a methanol/air and an ethanol/air spray flame. Detailed combustion mechanisms are implemented through the spray flamelet model. The

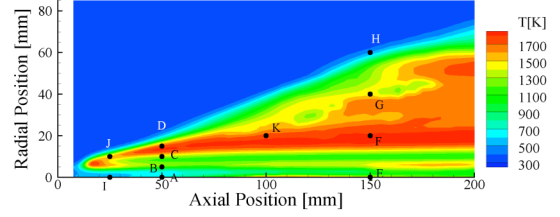


Fig. 1: Contour plot of gas temperature, marked positions show where PDFs are evaluated.

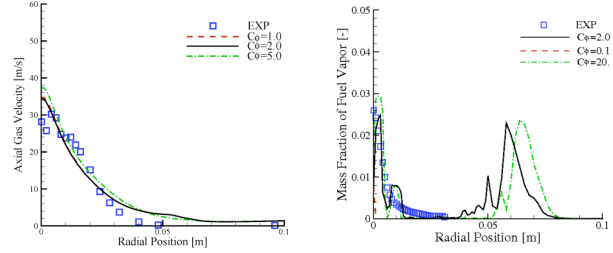


Fig. 2: Contour plot of gas temperature, marked positions show where PDFs are evaluated.

laminar spray flamelet library [21] has been pre-calculated using detailed transport and a detailed chemical reaction mechanism with 23 species and 168 elementary reactions [24] for methanol/air and 38 species and 337 elementary kinetic reactions [24] for ethanol/air.

Methanol/Air Spray Flame

A steady, two-dimensional, axi-symmetric, reactive turbulent liquid jet without swirl is modeled. A dilute methanol spray is injected into the turbulent air. Experiments have been performed by McDonell and Samuelsen [23], and the results are available for comparison with the simulations. The spray burner is described in detail in [23]. The experimental data at $x = 7.5$ mm are taken as inlet profiles for numerical computations. The measurements at the other experimental positions are compared with the numerical results.

Figure 1 shows the contour plot of the gas temperature computed by the joint mixture fraction - enthalpy PDF method. The gas temperature plot reveals some corrugation of the flame front as well as a cold spray core. In the regime near the axis where the spray evaporates, there is a cold region due to vaporization, and the flame resides in the mixing layer.

Figure 2 displays the experimental and numerical results of the mean gas velocity (left) and the methanol vapor mass fraction (right). The left part of Fig. 2 shows that the results of the PDF method are in good agreement with the experimental data. The mixing model constant, C_ϕ , c.f. Eqs. (4)-(5), has little influence on the gas velocity profiles. The results with $C_\phi = 1.0$ and $C_\phi = 2.0$ are almost identical, while the results with $C_\phi = 5.0$ are slightly different. Improvement

would be obtained if the velocity field in the PDF results were computed from a joint velocity - mixture fraction PDF model instead of the $k-\varepsilon$ model [19]. Unfortunately, there are no experimental values of the fuel vapor mass fraction at higher distances of the centerline where the simulations predict a second peak. It is difficult to judge from the methanol vapor plots whether the results with the standard or the modified model constant are better. Therefore, all following results are produced using the standard value 2.

Figure 3 shows contour plots of the joint mixture fraction – enthalpy PDF at various positions, c.f. Fig. 1. Position I resides at the central line where mixing is just initiated, the mean value of the mixture fraction is about 0.03 as can be seen from the figure. At this position, the mixture fraction and enthalpy are statistically independent. The samples of gas phase enthalpy show a wide range of values between -4 kJ/g and almost zero which is contributable to the evaporation of droplets in this region. The mixture fraction and the enthalpy are far away from being statistically independent at position B, which is located in the main regime of both evaporation and combustion. This is also true for position D shown in Fig. 3, which locates in the area of the turbulent mixing inside the boundary layer. A linear dependence of the mixture fraction and the enthalpy is found at the position K. Evaporation of droplets is completed and combustion and mixing associated with an almost linear variation of both mixture fraction and enthalpy is found. The figures clearly demonstrate that we find the entire range of correlation coefficient between zero and unity. Therefore, the commonly used assumption of statistical independence is anything but justified, in particular, if spray flames with their strong coupling of evaporation and combustion are considered.

Figure 4 shows a comparison of the transported PDF and the presumed PDFs at various positions. It is obvious that the bimodal shape cannot be represented by

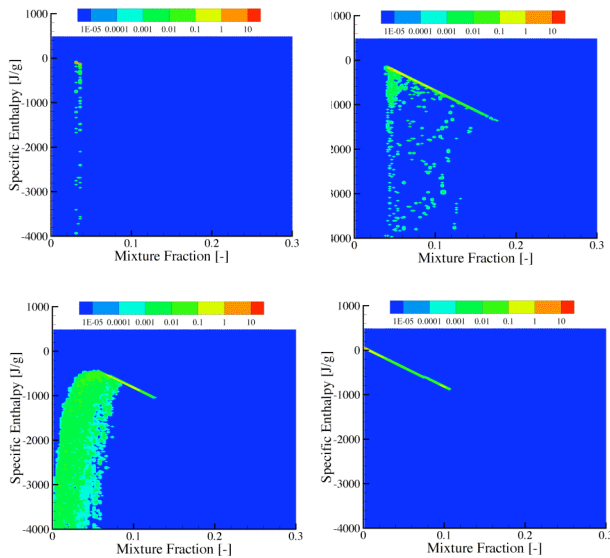


Fig. 3: Joint PDFs of mixture fraction and enthalpy at positions I (top left), B (top right), D (bottom left), and K (bottom right).

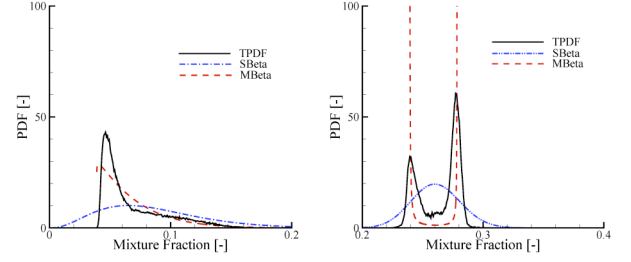


Fig. 4: Comparison of the transported PDF, the standard b PDF, and modified b PDF of the mixture fraction at positions B (left) and C (right).

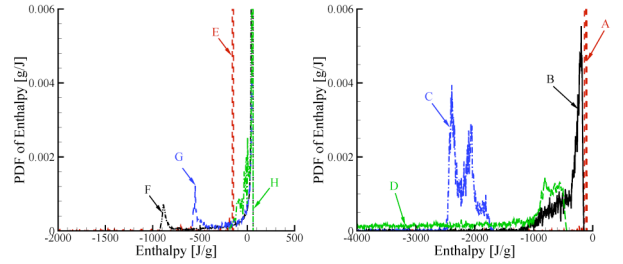


Fig. 5: Marginal PDF of the gas enthalpy at various positions. Left: $x = 50$ mm. Right: $x = 150$ mm.

the standard β function,

$$P(\xi_c) = \frac{\Gamma(\alpha + \beta)}{\Gamma(\alpha)\Gamma(\beta)} \xi_c^{\alpha-1} (1 - \xi_c)^{\beta-1}. \quad (6)$$

The standard β function assumes that the maximum value is unity and the minimum value is zero, which is not true in evaporating spray flows [18]. The present study reveals that the same situation occurs under reactive conditions. The modified β function suggested in [18] for non-reactive spray flows,

$$P(\xi_c) = \frac{\Gamma(\alpha + \beta)}{\Gamma(\alpha)\Gamma(\beta)} (\xi_{c,\max} - \xi_{c,\min})^{1-\alpha-\beta} \times (\xi_c - \xi_{c,\min})^{\alpha-1} (\xi_{c,\max} - \xi_c)^{\beta-1}, \quad (7)$$

introduces another two parameters to describe the bounds of the local mixture fraction, $\xi_{c,\min}$ and $\xi_{c,\max}$. The modified β function gives better approaches to the PDFs computed using Monte-Carlo method. Unfortunately, the physical meanings of the parameters $\xi_{c,\max}$ and $\xi_{c,\min}$ is not yet clear. Therefore, it is difficult to construct physical models for them. This task will be pursued in the future investigations.

The second marginal distribution of the joint PDF is the enthalpy shown in Fig. 5. It is seen that the peaks from positions A-B-C-D and F-G-E-H are reversed due to the energy consuming evaporation of droplets. The profiles of enthalpy are coarser due to the high values of enthalpy compared to the mixture fraction.

The present model is able to predict the pollutant emission. Figure 6 shows contour plots of carbon monoxide (left) and carbon dioxide (right) mass fraction. A comparison of Fig. 6 with the gas temperature contour plot displayed in Fig. 1 shows that carbon monoxide does not persist in the highest

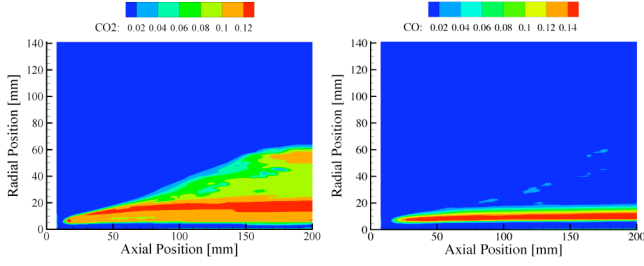


Fig. 6: Contour plot of the carbon monoxide (left) and carbon dioxide (right) mass fractions.

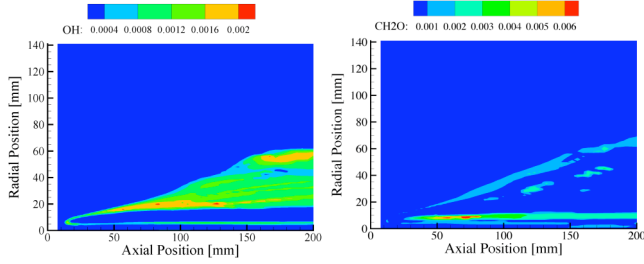
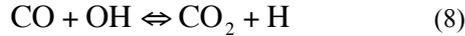


Fig. 7: Contour plot of the hydroxyl radical (left) and formaldehyde (right) mass fractions.

temperature regimes but in more moderate temperature areas whereas CO_2 prevails in high-temperature regions. This is due to the fact that the major chemical reaction being responsible for the consumption of CO is



with a very high activation energy. In fact, this reaction is the rate controlling chemical reaction step.

Figure 7 shows the OH radical on the left-hand side. Here it is obvious that OH is consumed in the region where CO persists. Typically, the OH attains maximum values in regimes where gas temperature attains high values. OH is sometimes used as an indicator for the flame position, and it is accessible to experimental methods, in particular, to laser induced fluorescence (LIF). Here the OH is consumed in the region where CO attains its maximum values. This is a result of the overall stoichiometry of the flame. The equivalence ratio equals three, and the fuel rich flame has CO in excess compared to OH so that the reaction in Eq. (7) is retarded. The right hand side of Fig. 7 shows the formaldehyde contour plot, and it is seen that it prevails in moderate temperature areas, which is typical for this species.

Ethanol/Air Spray Flame

A spray jet flame burner has been set up to investigate the ethanol flame [25]. Compared to a conventional simple jet flame burner, it has no bluff body and no pilot flame for stabilization to facilitate numerical computations. The obstructions caused by the fluid mechanics are avoided. The nozzle produces a hollow-cone spray. A multi-hole plate around the nozzle generates a homogeneous co-flow. A stable flame was

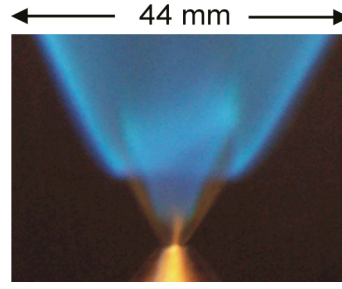


Fig. 8: Photograph of the spray flame

obtained by pre-heating the ethanol to 45°C at the nozzle exit. The air co-flow velocity was varied between 0 and 0.64 m/s. Close to the nozzle exit, the droplet size distribution and droplet velocity distribution of a non-reactive ethanol/air spray without co-flow are measured using phase Doppler anemometry (PDA). The gas temperature in an ethanol/air spray flame is measured using multi-line laser-induced fluorescence technique. The case of injection pressure $p = 2.0$ bar is used for the comparison of experiment and simulation. A joint enthalpy and mixture fraction PDF model is employed to simulate the ethanol/air spray flame.

Figure 8 shows the photograph of the spray flame, which has two separate reaction zones. Different from other spray burners where the two reaction zones are formed due to recirculation zone, the inner flame and outer flame are the results of different evaporation and combustion stages. Part of the liquid ethanol vaporizes immediately after atomization. The ethanol vapor mixes with the entrained air, and then the inner flame develops. The remaining ethanol droplets penetrate the surrounding airflow. When the expanding inner flame front gets close enough to the spray, evaporated fuel is ignited by hot products of the inner flame; thus, the wing-like outer flame is formed.

Figure 9 shows the contour plot of the time-averaged gas-phase temperature field from NO-LIF measurement and PDF simulation. The wing-like flame structure is predicted in the simulation. However, discrepancies are observed regarding the location of the outer flame kernel. The experiment shows that the kernel of the outer flame develops with an open angle, while the present method predicts a vertical flame kernel. This may be due to the coarse droplet size and velocity distribution in the experimental data. The distribution of droplet size and axial velocity used in the present computation for initial conditions has assumption, which is plausible in the non-reactive case, is

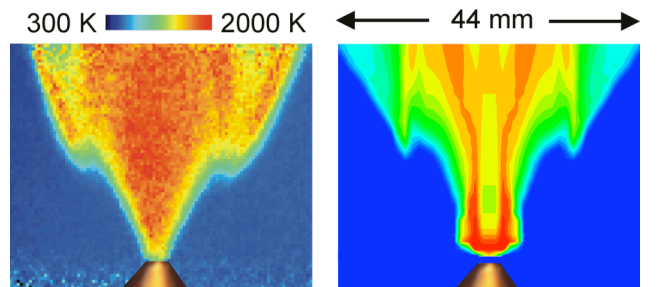


Fig. 9: NO-LIF measurements (left) and numerical simulation (right) of gas temperature

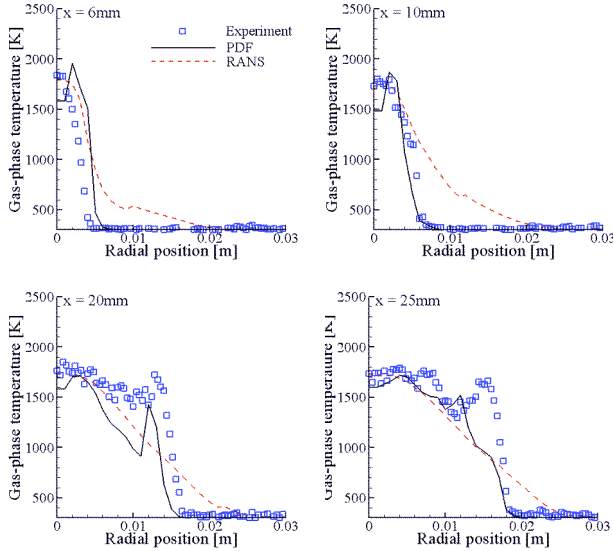


Fig. 10: Radial profiles of gas-phase temperature

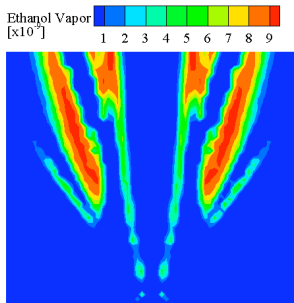


Fig. 11: Contour plot of the ethanol vapor mass fraction

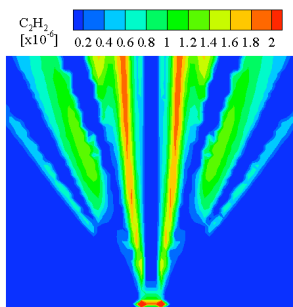


Fig. 12: Contour plot of the mass fraction of acetylene.

questionable in the reactive case where the interaction of spray and flame is significant. Figure 10 shows the profiles of the gas-phase temperature at different heights above the nozzle: $x = 6\text{mm}$, 10mm , 20mm , and 25mm . Symbols are the measurement of multi-line NO-LIF. The solid lines indicate the numerical results of the present PDF method. The dashed lines indicate the numerical results of RANS modeling [25]. The PDF method gives considerably better agreement than the RANS modeling. The hot wings of the spray flame are predicted by the PDF method (c.f. the section $x = 20\text{mm}$). RANS modeling over-predicts the flame width, and it fails to predict the two reaction zones. According to the experimental data, the temperature gradients at the edge of the flame are very high. This phenomenon is well predicted by the PDF method, whereas the RANS modeling gives smoother and flatter profiles. Discrepancies in the PDF modeling mainly result from the unknown liquid flux and turbulence quantities at the inlet profile. The predicted temperature profile at the

section $x = 6\text{mm}$ is broader than the experimental data. It may be due to the $k-\epsilon$ model, which usually over-predicts the spreading speed of the jet flow [4].

Figure 11 shows the computed mass fraction of ethanol vapor. The physical width of the plot is 60mm . Near the nozzle, part of the ethanol evaporates immediately. The vapor mixes and reacts with the entrained air, forming the inner flame. The remaining spray particles move and evaporate simultaneously. Ethanol vapor from this stage mixes with the entrained air and enhances the inner flame. When the temperature around the penetrated spray is high enough, the remaining spray evaporates faster. A considerable amount of ethanol vapor is formed and ignited by the inner flame. Then the outer flame develops.

Figure 12 displays the corresponding plot of the mass fraction of acetylene. Soot precursors typically are products of the buildup process of acetylene, an intermediate product of fuel pyrolysis. Although some precursors may be formed via fast cluster growth of polycyclic aromatic hydrocarbons (PAHs), the evidence suggests that formation via fast polymerization of polyenes or formation directly from acetylene could be important pathways as well [26]. Apparently, the formation mechanism of acetylene is much simpler than PAHs. Therefore, acetylene is widely used as soot precursor in soot modeling, especially in engineering modeling [27]. Simplified models, such as Hiroyasu's two-step soot model [28], takes fuel vapor as soot precursor. Many phenomenological soot models (e.g. [29]) take acetylene as soot precursor, if a single global reaction of fuel pyrolysis leading to acetylene is included [29], or acetylene has been considered in the chemical reaction mechanism as the present ethanol/air combustion mechanism does. Therefore, the present model is suitable for future soot modeling in the turbulent spray flames. The profile of acetylene is similar to that of ethanol vapor, which implies that acetylene is only formed where the equivalence ratio is relatively high. This is also part of the reason why Hiroyasu's model is applicable. Some differences in the profiles of ethanol fuel and acetylene can be observed. For instance, acetylene shows a more homogeneous distribution than ethanol vapor, i.e., the spatial gradient of ethanol vapor is higher; near the nozzle, there is little ethanol vapor predicted while acetylene does. These features will result in different performance of the soot models using fuel vapor or acetylene as soot precursor. As discussed before, acetylene as soot precursor has a solid physical meaning. The models using acetylene instead of ethanol vapor as soot precursor are more reliable, and their correct prediction is required.

Conclusions

A joint mixture fraction – enthalpy PDF transport equation has been derived and modeled for the simulation of turbulent spray flames. It is coupled with RANS equations and with the flamelet model for turbulent diffusion flames where laminar spray flamelet libraries are employed. It appears that commonly used

assumptions of statistical independence or linear dependence are not justified for mixture fraction and enthalpy. A comparison with experiment and previous RANS computations demonstrates the great improvement with the present model. Moreover, its ability to predict pollutant formation in spray flames is presented.

Acknowledgements

The authors acknowledge financial support of Deutsche Forschungsgemeinschaft (DFG) through the International Graduate College 710. H.-W. Ge thanks the National Natural Science Foundation of China for partial financial support under Grant No. 50506028.

References

1. S.B. Pope. PDF methods for turbulent reactive flows. *Prog. Energy Combust. Sci.* **11**, 119-192, 1985.
2. S.B. Pope. Lagrangian PDF methods for turbulent flows. *Annu. Rev. Fluid Mech.* **26**, 23-63, 1994.
3. C. Dopazo. Recent developments in pdf methods. In *Turbulent Reacting Flows*, P.A. Libby and F.A. Williams, Eds, Academic Press London, 1994.
4. S.B. Pope. *Turbulent Flow*. Cambridge University Press, Cambridge, 2000.
5. R.W. Bilger, S.B. Pope, K.N.C. Bray, and J.F. Driscoll. Paradigms in turbulent combustion research. *Proc. Combust. Inst.* **30**, 21-42, 2005.
6. W.P. Jones and D.H. Sheen. A probability density function method for modelling liquid fuel sprays. *Flow Turbul. Combust.* **63**, 379-394, 1999.
7. M. Zhu, K.N.C. Bray, and B. Rogg. PDF modeling of spray autoignition in high pressure turbulent flows. *Combust. Sci. Technol.* **120**, 357-379, 1996.
8. M.S. Raju. Application of scalar Monte Carlo probability density function method for turbulent spray flames. *Numer. Heat Transfer A* **30**, 753-777, 1996.
9. M.S. Raju. Scalar Monte-Carlo PDF computations of spray flames on unstructured grids with parallel computing. *Numer. Heat Transfer B* **35**, 185-209, 1999.
10. P. Durand, M. Gorokhovski, and R. Borghi. An application of the probability density function model to diesel engine combustion. *Combust. Sci. Technol.* **158**, 47-78, 2000.
11. C. Taut, C. Correa, O. Deutschmann, J. Warnatz, S. Einecke, C. Schulz, and J. Wolfrum. 3D-modelling with Monte-Carlo-PDF methods and laser diagnostics of the combustion in a two-stroke engine. *Proc. Combust. Inst.* **28**, 1153-1159, 2000.
12. M.S. Raju. On the importance of chemistry-turbulence interactions in spray computations. *Numer. Heat Transfer B* **41**, 409-432, 2002.
13. M. Zhu and K. N. C. Bray and O. Rumberg and B. Rogg. PDF transport equations for two-phase reactive flows and sprays. *Combust. Flame* **122**, 327-338, 2000.
14. O. Rumberg and B. Rogg. Full PDF modelling of reactive sprays via an evaporation-progress variable. *Combust. Sci. Technol.* **158**, 211-247, 2000.
15. Z.-H. Liu, C.-G. Zheng and L.-X. Zhou. A joint PDF model for turbulent spray evaporation/combustion. *Proc. Combust. Inst.* **29**, 561-568, 2002.
16. B. Naud. PDF modeling of turbulent sprays and flames using a particle stochastic approach. *PhD Thesis*, Delft University of Technology, Delft, Netherland, 2003.
17. C. Hollmann and E. Gutheil. Flamelet-modeling of turbulent spray diffusion flames based on a laminar spray flame library. *Combust. Sci. Technol.* **135**, 175-192, 1998.
18. H.-W. Ge and E. Gutheil. Probability density function (PDF) simulation of turbulent spray flows. *Atomiz. Sprays* **16**, 531-542, 2006.
19. H.-W. Ge and E. Gutheil, Joint velocity-scalar PDF modeling of turbulent spray flows. *Proc. 20th Annu. Conf. ILASS-Europe*, Orléans, France, Sept. 2005.
20. C. Hollmann and E. Gutheil. Modeling of turbulent spray diffusion flames including detailed chemistry. *Proc. Combust. Inst.* **26**, 1731-1738, 1996.
21. E. Gutheil and W. A. Sirignano. Counterflow spray combustion modeling including detailed transport and detailed chemistry. *Combust. Flame* **113**, 92-105, 1998.
22. E. Gutheil. Structure and extinction of laminar ethanol/air spray flames. *Combust. Theory Modelling* **5**, 131-145, 2001.
23. V.G. McDonell and G.S. Samuelsen. An experimental data base for computational fluid dynamics of reacting and nonreacting methanol sprays. *J. Fluids Engin.* **117**, 145-153, 1995.
24. C. Chevalier. Entwicklung eines detaillierten Reaktionsmechanismus zur Modellierung der Verbrennungsprozesse von Kohlenwasserstoffen bei Hoch- und Niedrigtemperaturbedingungen. *PhD Thesis*, University Stuttgart, Stuttgart, Germany, 1993.
25. I. Düwel, H.-W. Ge, H. Kronemayer, R. W. Dibble, E. Gutheil, C. Schulz, and J. Wolfrum. Experimental and numerical characterization of a turbulent spray flame. *Proc. Combust. Inst.* **31**, 2247-2255, 2007.
26. P.A. Tesner, I.Y. Evplanova, and S.V. Shurupov. Soot formation in isothermic pyrolysis of mixtures of various hydrocarbons. *Kinetics Catalysis* **41**, 183-185, 2000.
27. I.M. Kennedy. Models of soot formation and oxidation. *Prog. Energy Combust. Sci.* **23**, 95-132, 1997.
28. H. Hiroyasu and K. Nishida. Simplified three-dimensional modeling of mixture formation and combustion in a D.I. diesel Engine. *SAE Technical Paper* **890269**, 1989.
29. F. Tao, D.E. Foster, and R.D. Reitz. Soot structure in a conventional non-premixed diesel flame. *SAE Technical Paper* **2006-01-0196**, 2006.